ELSEVIER

Ultrasonics 36 (1998) 1–6

Ultrasonics

Advances in ultrasonic electrostatic transduction

D.A. Hutchins [a,*], D.W. Schindel [b], A.G. Bashford [a], W.M.D. Wright [a]

[a] *Department of Engineering, University of Warwick, Coventry, CV4 7AL, UK*
[b] *Institute for Aerospace Research, National Research Council, Ottawa, Ont., K1A OR6, Canada*

Abstract

This paper describes some recent advances in the use of electrostatic transducers for performing ultrasonic measurements in both air and water. It will be shown that through-transmission imaging can be performed in metals, polymers and fibre-reinforced composites. Also possible are various forms of imaging in air, including tomographic reconstruction of flow and temperature fields in gases. © 1998 Elsevier Science B.V.

Keywords: Ultrasonic; Capacitance; Electrostatic; Transducers; Air-coupled

1. Introduction

There has been increased interest in the use of ultrasonic transducers in air in recent years. This has arisen mainly because of the problems associated with some non-destructive evaluation (NDE) methods, where rapid scanning of large areas is required. Other potential applications include flow measurement, position sensing in robotics and others. In many such cases, it is important to develop methods that can operate with a reasonable sensitivity, but with as wide a bandwidth as possible.

There are several approaches that can be used to design transducers that operate in air [1], but two of these are used most widely: piezoelectric and electrostatic transducers. In piezoelectric designs, the main problem is to overcome the large acoustic impedance mismatch between the piezoelectric ceramic and air. This can be achieved using impedance matching layers, and the response is also improved if a piezocomposite active element is designed appropriately. These are often in the form of 1–3 connectivity composites [2], and such devices have been shown to give good results in NDE experiments [3]. Because of the need to design impedance matching layers for specific frequencies, the result is often a transducer that is fairly resonant.

Electrostatic devices have been investigated for some years, and their response has been both modelled theoretically and measured experimentally [4–6]. Early devices used earlier roughened backplates or metallic plates containing V-grooves, against which a thin polymer membrane was placed. These devices were shown to be dependent on the surface features present on the rigid backplate, and also on the polymer membrane properties. As a source, the flexible membrane experiences a force under an applied signal voltage, but the devices can also be used as receivers in the presence of an applied d.c. bias voltage. Various studies have been reported on the response of electrostatic devices, but it has been found that an important feature is the careful control of backplate geometry in terms of surface condition. For these reasons, various workers suggested that the use of silicon micromachining techniques would be a good way of maintaining reproducible surface features [7,8]. The devices used in this paper follow this approach [8], as have various other designs which have been described in the literature [6–9]. There are two basic possibilities in micromachining. The backplate can be machined separately to obtain the required surface features, and a flexible polymer membrane applied subsequently to obtain the full structure – this is the approach adopted here. Conversely, micromachining can be used to construct the whole devices which typically have a silicon nitride or polysilicon membrane [9,10]. The advantage of a thin polymer membrane is that the result is a transducer with a wide bandwidth which at present does not seem possible with fully micromachined devices. Polymer membrane devices have many advantages and have been used for several applications, including imaging and materials characterisation [11–16].

* Corresponding author. Tel: (44) 1203 523874; fax: (44) 1203 418922; e-mail: dah@eng.warwick.ac.uk

PII S0041-624X(97)00079-6

In the following, the devices using polymer membranes will be described briefly in terms of their construction and properties in air. This is then followed by a series of experiments, involving the inspection of metals and polymers in air, various forms of air-coupled imaging, and the measurement of temperature and flow fields in gases.

2. Device construction and performance

A schematic diagram of a micromachined silicon backplate transducer is shown in Fig. 1. The backplate contains 40 μm diameter cylindrical pits, regularly-spaced across the aperture. This is coated with gold to make it conducting. A thin insulating Kapton membrane, usually in the 5–10 μm range in thickness, is then applied to the backplate under the influence of a d.c. bias voltage. This traps air in the cylindrical holes, forming an air-spring. An evaporated electrode on the outer membrane surface acts as the ground plane, and generation and detection signals are obtained via connection to the conducting backplate. A grounded case completes the device, and acts a shield against external r.f. noise.

A typical signal detected in air from a device with a 10 mm active diameter is shown in Fig. 2(a) and was obtained by excitation with a transient voltage from a commercial Panametrics pulser unit. As can be seen, the time waveform is well-damped, with none of the resonant characteristics usually present in alternative piezoelectric and fully micromachined devices. This is confirmed in the FFT of the signal, presented in Fig. 2(b), where a reasonable response up to 2 MHz can be seen. From other tests, it appears that the device acts approximately as a plane piston, without too many complications from variations in amplitude and phase across the aperture. This is evident from the beam plot in air, presented in Fig. 2(c), which shows the spatial changes in amplitude of the wide bandwidth pulse shown in Fig. 2(a). Note the rapid decay of the signal with

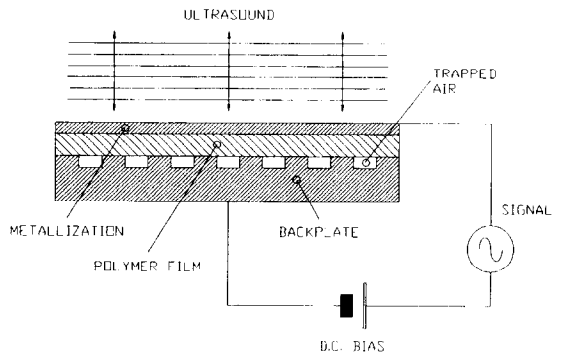

Fig. 1. Schematic diagram of a micromachined backplate electrostatic transducer.

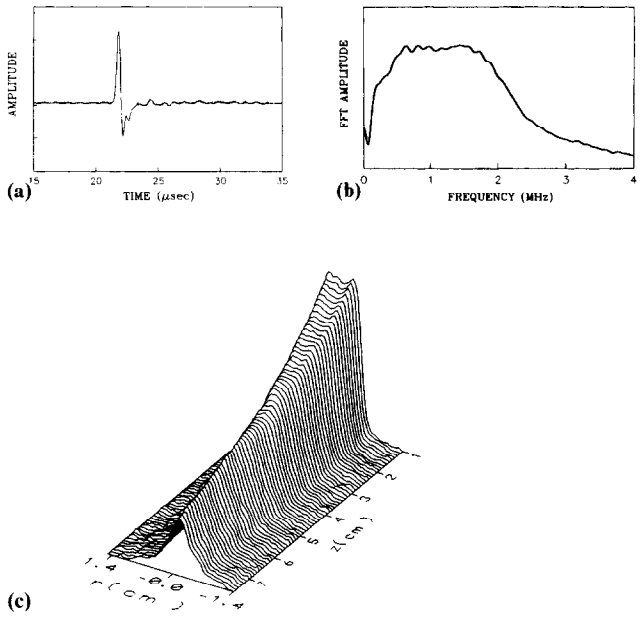

Fig. 2. (a) Typical received waveform in air, and (b) spectrum that resulted following an FFT of the time waveform, for a 10 mm diameter electrostatic transducer excited by a transient from a Panametrics pulser unit. (c) The resultant beam profile in air, measured using a scanned miniature hydrophone.

distance, which is due to the high attenuation of signals in air at frequencies above 1 MHz. As this attenuation is frequency dependent, the bandwidth reduces with distance away from the transducer. It is evident, however, that the beam is well-behaved, with the edge-wave components visible at small distances from the source, and a highly collinated beam. This is aided by the short-wavelengths in air, leading to a high aperture to wavelength ratio.

3. Through-transmission experiments

The devices are sufficiently sensitive that signals can be transmitted through solid plates in air, despite the high signal loss caused by their insertion between a source/receiver pair. The source was excited with the Parametric pulser, and the receiver connected to a Cooknell CA6C charge amplifier, which also provided a d.c. bias to the detector. Typical results are shown in Fig. 3 for three thicknesses of carbon fibre-reinforced composites. As will be seen, reasonable time waveforms are obtained in through-transmission, all of which appear to have a resonant nature. This arises because the parallel plate effectively selects the through-thickness resonant frequency, which is the condition for maximum transmission through the plate in air. The effect of increased thickness is then to reduce the resonant frequency, as is seen in the time waveforms. Note that an FFT of such time waveforms leads to a frequency

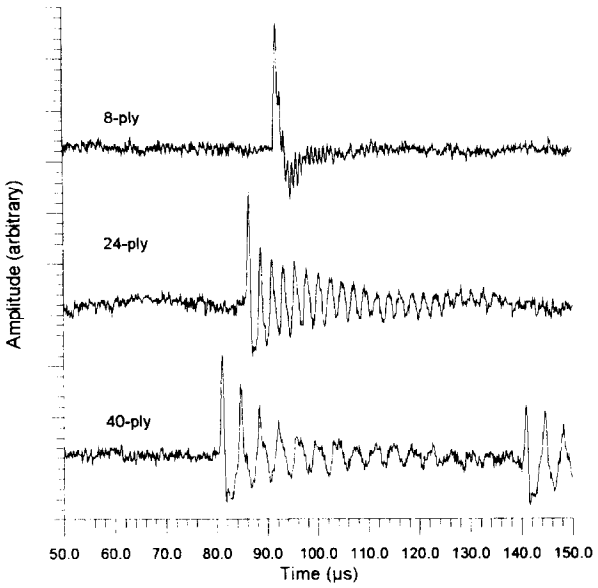

Fig. 3. Air-coupled waveforms in 8-ply, 24-ply and 40-ply thick quasi-isotropic carbon-fibre-reinforced polymer plates.

measurement which can be used for materials characterisation [12].

It is possible to form images of internal defects by scanning the source/receiver pair over the plates in through-transmission mode. This has been performed for a square artificial defect of 6.35 mm width, formed by including Teflon layers in a 2.2 mm thick (16-ply) carbon fibre composite, and for damage caused by impact. The results are shown in Fig. 4(a) and (b). The images clearly show the region of damage, with the known position of the defect being shown in Fig. 4(a) as the dotted line, and the area of impact being similarly identified in Fig. 4(b). These images were formed by monitoring the amplitude of the through-transmitted signal at the resonant frequency of the plate, as a function of position. For a defect-free region, a good signal amplitude is obtained, whereas in the presence of artificial and real defects the resonance is no longer present. In fact, experiments show that the presence of the resonance is a very sensitive method of detecting small changes in condition of the sample.

Other examples are seen in metal plates, where now the acoustic impedance of the material is greater than a polymer-based composite, and hence where transmitted signals are of lower amplitude. An example is shown for aluminium in Fig. 5 for two plate thicknesses, where a resonance is observed in the thinner plate, but where separate multiple reflections of the wide bandwidth pulse are visible in the thicker material. Although such signals are not of large amplitude, it is still possible to perform imaging. This is shown in Fig. 6, where through-transmission imaging has been used to detect an 8 mm circular artificial defect in 0.7 mm thick aluminium plate. The defect was in the form of a change in thickness to

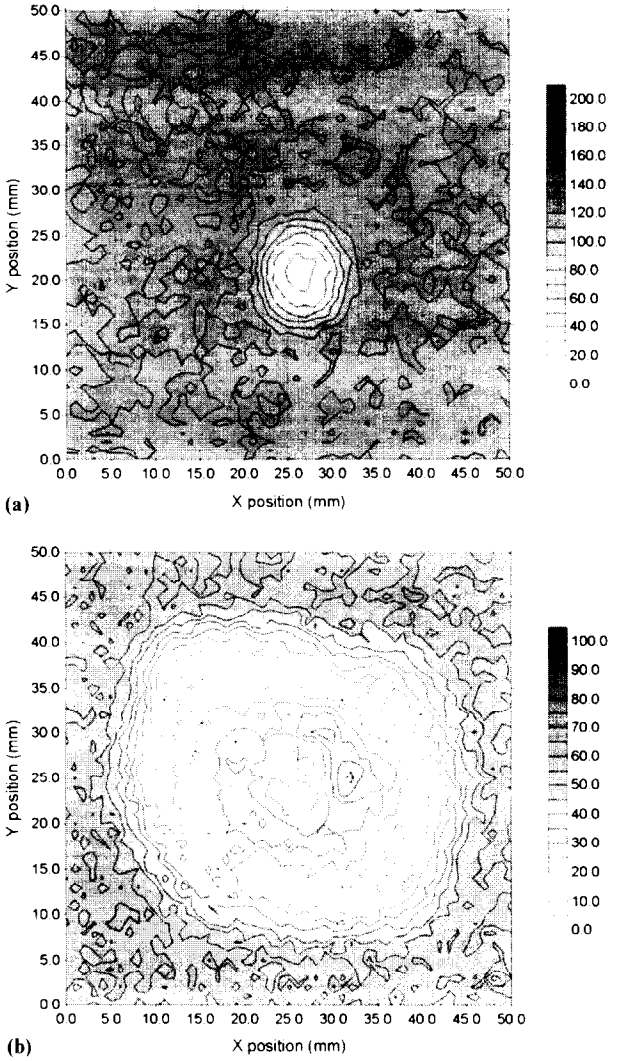

Fig. 4. Images formed by through-transmission scanning of a 16-ply thick quasi-isotropic composite plate containing (a) a 6.35 mm wide artificial Teflon defect, and (b) impact damage.

0.35 mm, i.e. the thickness had been reduced to one half of the original value. Two images are shown, formed by detecting (a) the received waveform amplitude in mV, and (b) the change in time of arrival. In both cases, the defect is visible, but it appears that the time of arrival is the more sensitive detection method.

A final example of through-transmission experimentation is the testing of materials at elevated temperatures. In experiments, we have demonstrated that electrostatic transducers can be constructed which can operate at various temperatures. For instance, with the use of Kapton films, measurements in air up to 200°C are possible. This has application in measurements of polymer based materials, where the softening of the material can be observed by a large change in the acoustic velocity. Note that, being a non-contact method, such materials can be observed at temperatures up to their melting point. Another examples of a useful measure-

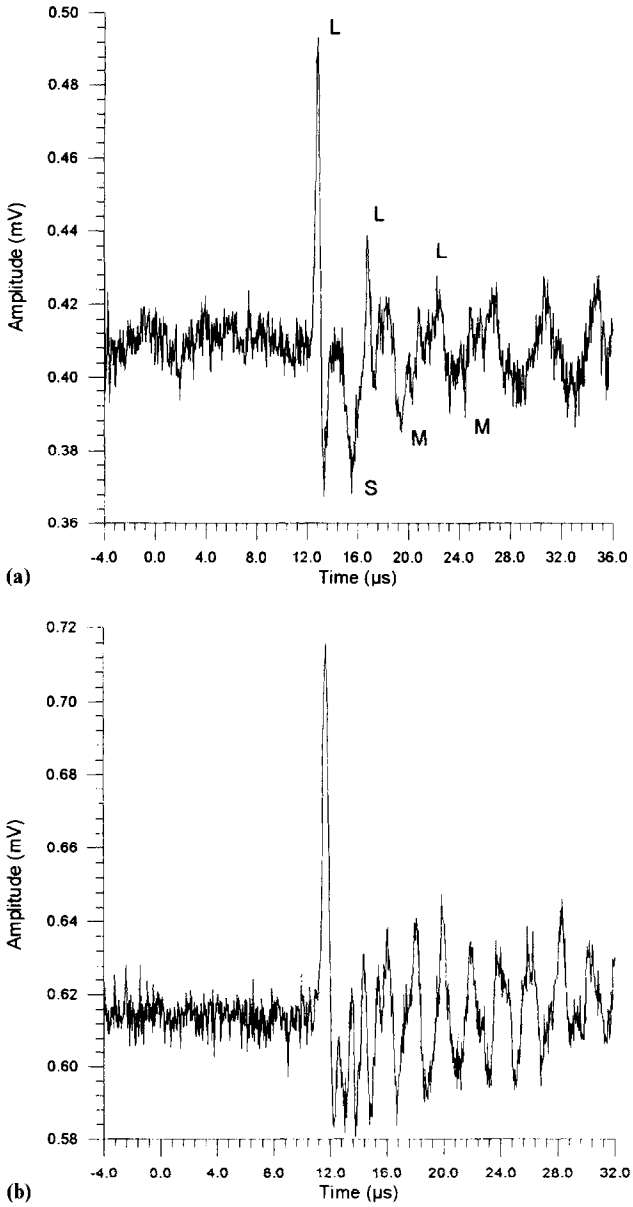

Fig. 5. Through-transmission waveforms in aluminium plates of thickness (a) 12.9 mm and (b) 6 mm.

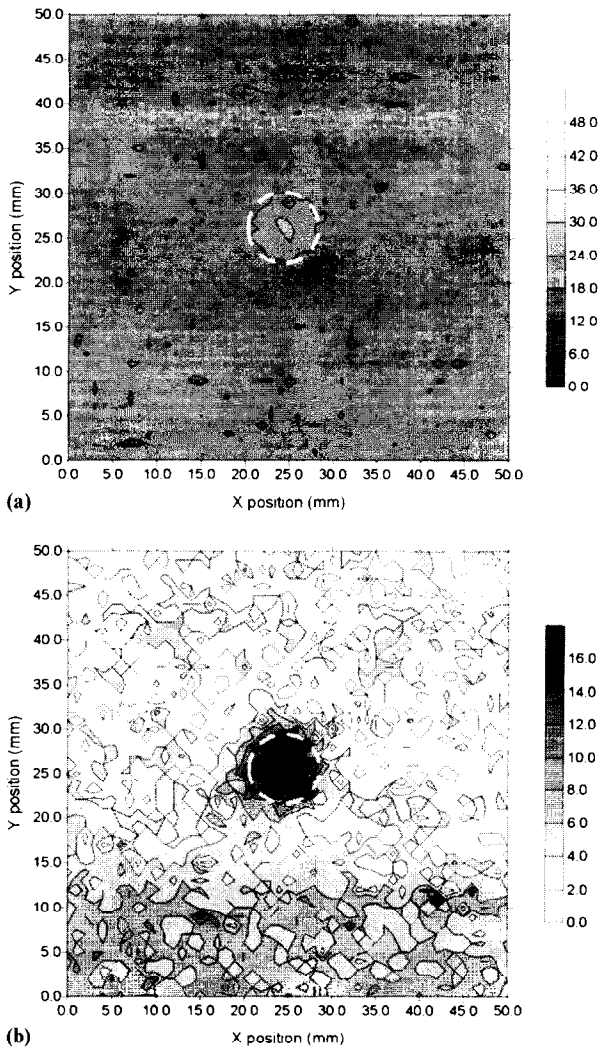

Fig. 6. Through-transmission imaging of an 8 mm diameter defect machined halfway through a 0.7 mm thick aluminium plate. The image in (a) was formed from the received amplitude, and in (b) from the change in time of arrival at the receiver.

ment that can be made with such a system is the burn-out of polymer binder in injection-moulded ceramic materials, and is the subject of a present study.

4. Other forms of imaging

The polymer film electrostatic transducers have been shown to be of reasonable sensitivity, and hence other possibilities for imaging arise because of these properties. The first is conventional pulse-echo imaging, but now performed by reflection from solid surfaces with air as the coupling medium. This can be achieved with focused air-coupled piezoelectric probes, using an impedance matching layer. However, it was felt that the excellent properties of the planar devices described earlier could be used, together with an additional focusing element. Two possibilities were considered: use of a reflecting parabolic metal mirror, or the use of a zone plate. The latter was chosen, for several reasons. First, it would be less bulky, and would allow the transducers to be placed closer to the surface being imaged. In addition, the zone plate could be manufactured by micromachining techniques, in the same way as the transducer backplates, and placed close to the transducer aperture.

Fig. 7(a) shows the zone plate, which was micromachined from a stainless steel sheet. The transducer was excited at 580 kHz, to produce a spot size at the focus of $\cong 600$ μm, at a focal distance of 7.5 mm from the zone plate face. With the zone plate attached directly to the front of the transducer case, and aligned axially with the transducer aperture, the radiated field of the device is as shown in Fig. 7(b). This was obtained by scanning a

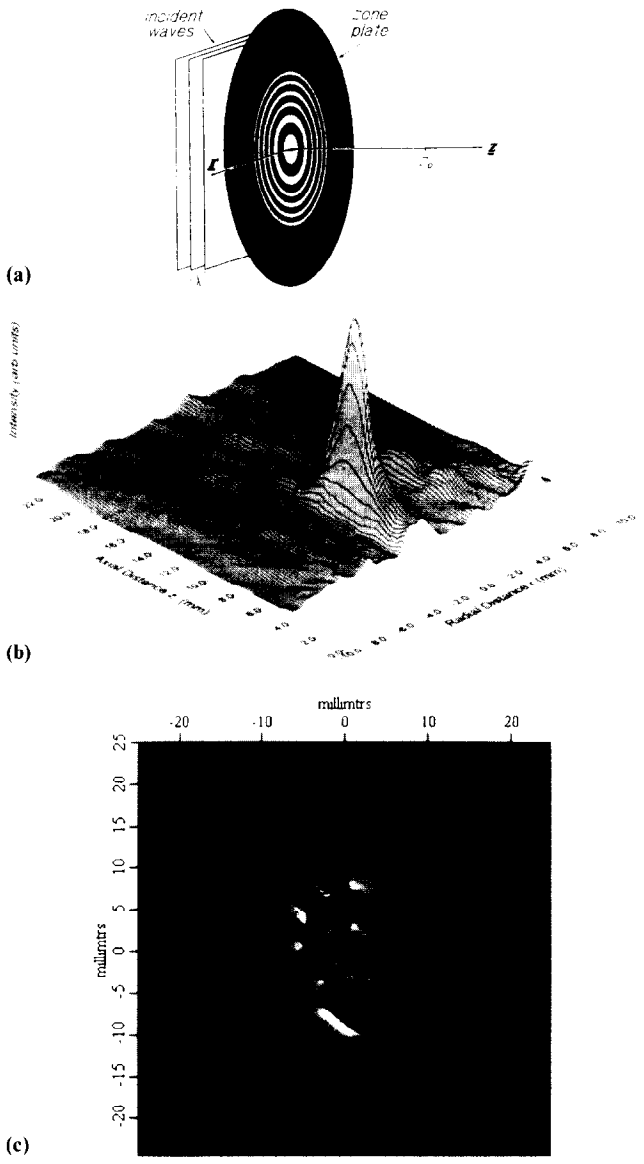

Fig. 7. (a) A micromachined zone plate, positioned in front of the transducer aperture to produce a focal region in air at a distance of 7.5 mm, at a frequency of 580 kHz. (b) The radiated field in a horizontal plane containing the transducer axis. (c) A reflected amplitude image of a Canadian coin.

miniature hydrophone in a horizontal plane containing the transducer axis, to obtain the spatial variations around the focal region. It is evident that a satisfactory focus had been achieved.

Reflection images were now obtained by placing surfaces and objects in the focal region of the zone plate, and by operating the transducer in a pulse-echo mode. To form the image, a RITEC gated tone burst amplifier was used in conjunction with a superheteordyned receiver to give low noise detection of reflected signals. The transducer was scanned over the surface of the sample, and images formed from the amplitude of the detected signal. This effectively detects surface topography features. To illustrate this system, Fig. 7(c) shows the image formed of a Canadian one-dollar coin, placed on a flat reflective surface. The result shows that excellent resolution is obtained. Such a system has many applications in the measurement of surface topography, and may be useful in replacing optical systems that are used for such measurements at present.

A second form of imaging is obtained from tomographic reconstruction techniques, applied to data taken by scanning a source/receiver pair in air across a single planar cross-section. In the preliminary experiments reported here, a pair of micromachined transducers were scanned as a series of projections in a horizontal plane, to conform with the geometry used for image reconstruction via filtered back-projection algorithms. The technique can be used to reconstruct spatial variations in any acoustic parameter that varies across the imaging plane. In the example shown here, flow variations were detected by measuring the acoustic velocity variations, caused by the passage of an air jet passing at an angle of approximately 45° through the image plane. The jet itself increases in cross-sectional area as it propagates away from the 1 mm diameter nozzle.

To illustrate the types of image that can be obtained, Fig. 8 shows the changes in acoustic velocity across the jet at a distance of 30 mm from the nozzle. It can be seen that there is a change in acoustic velocity, caused by air flow, which is easily detected by measuring the time of flight variations along multiple paths across the plane. Note that in this contour image, the elongation of the image is caused by the principle flow being at 45° to the scanning plane. While this image was obtained by simple time of flight measurements, the results correlate well with the predictions of fluid dynamics, where the change in acoustic velocity can be predicted from the flow conditions. More information is potentially available, in terms of temperature and flow variations,

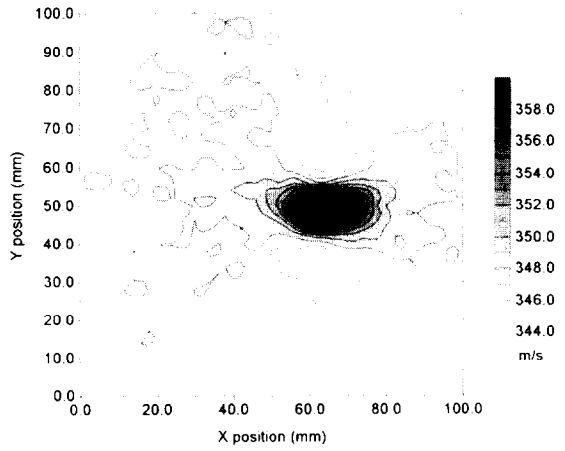

Fig. 8. Tomographic reconstruction of the change in sound velocity, caused by passage of an air jet at 45° to an image plane containing a source/receiver pair.

which in principle can be obtained simultaneously; this will be the subject of further work.

5. Conclusions

In this paper, we have covered some of the measurements and imaging methods that can be performed using micromachined electrostatic ultrasonic transducers. These are just some of the many applications of such devices. It is anticipated that with increased integration of electronics and sensor systems, the use of micromachining will become increasingly important in the design and manufacture of ultrasonic transducers, particularly for use in air.

Acknowledgement

This work was funded in part by the Engineering and Physical Sciences Research Council (ESPRC), UK.

References

[1] W. Manthey, N. Kroemer, V. Mágori, Meas. Sci. Tech. 3 (1992) 249.
[2] G. Hayward, A. Gachagan, J. Acoust. Soc. Am. 99 (1996) 2148.
[3] R. Farlowe, S. Kelly, G. Hayward, Proc. 1994 IEEE Ultrasonics Symp., 1994, p. 1099.
[4] W. Kuhl, G.R. Schodder, F. Schroder, Acustica 4 (1954) 519.
[5] H. Carr, C. Wykes, Ultrasonics 31 (1993) 13.
[6] M.J. Anderson, J.A. Hill, C.M. Fortunko, N.S. Dogan, R.D. Moore, J. Acoust. Soc. Am. 97 (1995) 262.
[7] K. Suzuki, K. Higuchi, H. Tanigawa, IEEE Trans. Ultrason. Ferro. Freq. Control 36 (1989) 620.
[8] D.W. Schindel, D.A. Hutchins, L. Zou, M. Sayer, IEEE Trans. Ultrason. Ferro. Freq. Control 42 (1995) 42.
[9] M.J. Haller, B.T. Khuri-Yakub, IEEE Trans. Ultrason. Ferro. Freq. Control 43 (1996) 1.
[10] P.C. Eccardt, K. Niederer, T. Scheiter, C. Hierold, Proc. 1996 IEEE Ultrasonics Symposium, pp. 959–962.
[11] D.W. Schindel, D.A. Hutchins, Ultrasonics 33 (1995) 11.
[12] D.A. Hutchins, W.M.D. Wright, D.W. Schudel, J. Acoustic. Soc. Am. 96 (1994) 1634.
[13] B. Hosten, D.A. Hutchins, D.W. Schindel, J. Acoust. Soc. Am. 99 (1996) 2116.
[14] D.W. Shindel, D.A. Hutchins, W. Grandia, Ultrasonics 34 (1996) 621.
[15] W.M.D. Wright, D.W. Shindel, D.A. Hutchins, J. Acoust. Soc. Am. 95 (1994) 2567.
[16] D.W. Schindel, D.S. Forsyth, D.A. Hutchins, A. Fahr, Ultrasonics 35 (1997) 1.